OPEN

Ocean acidification impacts mussel control on biomineralisation

Susan C. Fitzer, Vernon R. Phoenix, Maggie Cusack & Nicholas A. Kamenos

School of Geographical and Earth Sciences, University of Glasgow, Glasgow, G12 8QQ, UK.

Ocean acidification is altering the oceanic carbonate saturation state and threatening the survival of marine calcifying organisms. Production of their calcium carbonate exoskeletons is dependent not only on the environmental seawater carbonate chemistry but also the ability to produce biominerals through proteins. We present shell growth and structural responses by the economically important marine calcifier *Mytilus edulis* to ocean acidification scenarios (380, 550, 750, 1000 µatm $p\mathrm{CO}_2$). After six months of incubation at 750 µatm $p\mathrm{CO}_2$, reduced carbonic anhydrase protein activity and shell growth occurs in *M. edulis*. Beyond that, at 1000 µatm $p\mathrm{CO}_2$, biomineralisation continued but with compensated metabolism of proteins and increased calcite growth. Mussel growth occurs at a cost to the structural integrity of the shell due to structural disorientation of calcite crystals. This loss of structural integrity could impact mussel shell strength and reduce protection from predators and changing environments.

Atmospheric carbon dioxide emissions are expected to rise from present day values of 384 µatm to beyond 710–855 µatm to 855–1130 µatm by the year 2100[1,2]. Changes in carbonate chemistry resulting from absorbance of CO_2 into the oceans is not only reducing the pH of the seawater through ocean acidification (OA), but also reducing the oceanic carbonate saturation state (Ω)[2]. This has the potential to limit the ability of calcifying marine organisms to produce their protective exoskeletons and shells. Ocean acidification has been shown to have both positive and negative implications for marine calcifiers[3–6]. Specific proteins play key roles in biomineral formation e.g. in molluscs[7,8] and brachiopods[9,10] such as carbonic anhydrase[7] forming bicarbonate ($\mathrm{HCO_3}^-$) through the hydrolysis of CO_2[11]. Held within the calcium carbonate shell is an organic matrix (0.1–5% of the shells) comprising proteins, glycoproteins and chitin[7] which all have a function in the construction of the shell[7]. However, the details of the mechanisms or pathways involved within this process remain unclear. In addition to the importance of proteins in biomineral formation, the exquisite control on crystallographic orientation indicates the high level of biological control exerted on biomineral formation[9,10]. It is important to combine both physical and biological responses of marine organisms when trying to understand future implications of ocean acidification on marine organisms. Long-term and, if possible, multi-generational research is also needed to predict the possibility of acclimatisation and potential adaptation by marine organisms to future ocean acidification. However few such studies exist[12,13] because the difficulties in maintaining laboratory cultures mean that these are generally restricted to organisms with shorter life cycles.

The common blue mussel *Mytilus edulis* is an economically important food source; globally mollusc aquaculture comprises 23.6% (14.2 million tonnes) of an annual $119.4 billion industry[14]. *M. edulis* can be cultured within the laboratory and, importantly, the bimineralic shell enables investigation of the two major biogenic polymorphs of calcium carbonate: calcite (prismatic layer) and aragonite (nacreous layer, mother of pearl).

We examine the responses of *M. edulis* to four $p\mathrm{CO}_2$ concentrations (380, 550, 750 and 1000 µatm $p\mathrm{CO}_2$), over a 6 month incubation. These $p\mathrm{CO}_2$ concentrations represent future ocean acidification scenarios leading up to the year 2100[1]. Mussels were also exposed to combined increases in $p\mathrm{CO}_2$ and temperature (ambient plus 2°C) relating to future projected climate change[1]. Mussels were examined for shell structural and crystallographic orientation, growth, calcite and aragonite thickness and carbonic anhydrase concentration. The aim of the investigation was to determine the presence of any OA 'tipping' point or threshold, which once reached, may cause calcifiers to experience difficulties in maintaining control of biomineralisation and struggle to produce structurally sound shell growth.

Results & Discussion

Although mussel shell growth continued with increasing $p\mathrm{CO}_2$, their ability to control the shell ultrastructure was diminished (Figure 1 and 2). The growing edge of the new calcite deposited during 6 months growth at 380 µatm
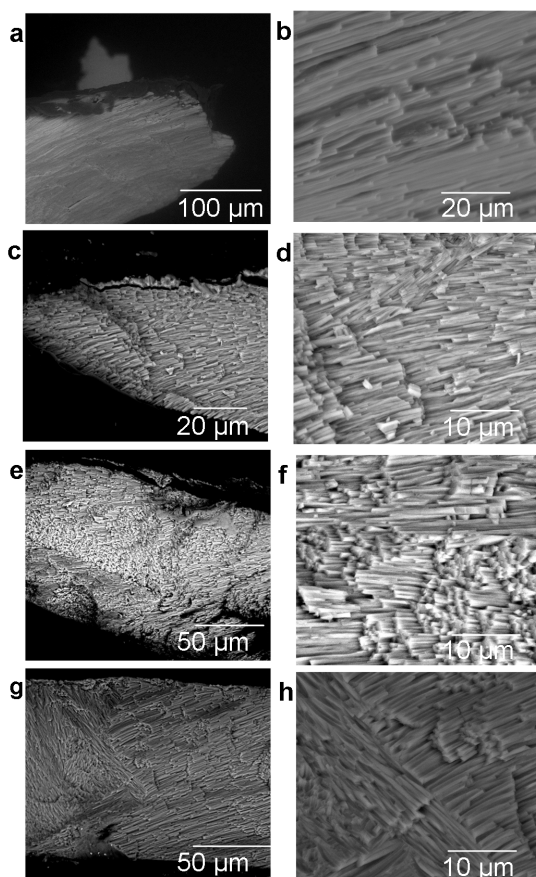
Figure 1 | Secondary electron images of new calcite growth in *M. edulis* shells after 6 months at 380, 550, 750 and 1000 µatm *p*CO₂, (a, b) 380 µatm, (c, d) 550 µatm, (e, f) 750 µatm, and (g, h) 1000 µatm, scale bars presented in µm. Images of uncoated samples acquired in environmental mode at 20 kV.

*p*CO₂ (Figure 1 (b)) had a uniform structural orientation with an average angle of 18.6° from the horizontal (calcite: aragonite interface) (Supplementary Table 1). New calcite crystal formation was disorientated in shells cultured for 6 months at 550, 750 and 1000 µatm *p*CO₂ compared to the 380 µatm *p*CO₂ control (Figure 2). Average degrees of spread of calcite crystals from the horizontal interface were 47.0°, 3.9° and 37.2° respectively for 550, 750 and 1000 µatm *p*CO₂ (Figure 1 (d), (f) and (h)) suggesting that projected climate change will impact shell structure (Figure 1). Crystallographic orientation pole figures confirmed changes in the spread of crystallographic orientations, suggesting further disorganisation of crystal structures, the degrees of spread were observed to be 20° for 380 µatm *p*CO₂ ambient (Figure 2 (a)), 40° for 550, 30° for 750 and 20° for 1000 µatm *p*CO₂. Disturbed ultrastructure was also observed in *Mytilus galloprovincialis*[15] after transference to acidified seawater at pH 7.3 compared to ambient at pH 8.1. Increasing culture temperature by ambient plus 2°C resulted in calcite crystals with more structural disorientation only at 750 µatm and 1000 µatm where the average calcite growth angle was 60.9° and 78.8° respectively, compared to new growth calcite crystal angle of 28.7° at 380 µatm *p*CO₂ and ambient plus 2°C (Figure 3 (b), (d) and (f)) (Supplementary Table 2). Crystallographic orientation pole figures also confirmed this with spread in the data from 20° at 380 µatm *p*CO₂ ambient plus 2°C, to 40° at 750 µatm *p*CO₂ ambient plus 2°C and 30° at 1000 µatm *p*CO₂ ambient plus 2°C. Thus a combination of projected temperature increases with synchronous OA further enhances the disorientation of the calcite structure. This could be as global warming increases standard metabolic rate reducing the
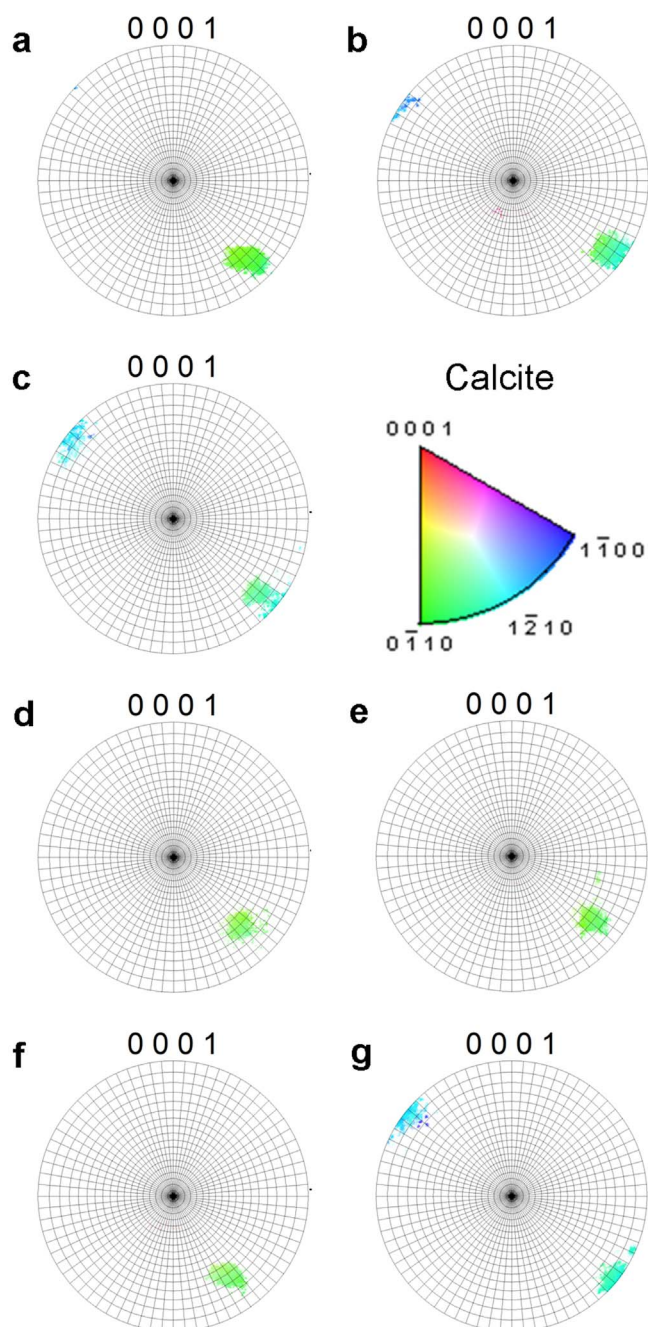

Figure 2 | Electron Back Scatter Diffraction (EBSD) crystallographic orientation calcite pole figure diagrams indicating the orientation angle of the calcite in the electron back scatter diffraction (EBSD) images (a) 380 µatm, (b) 380 µatm 12°C, (c) 550 µatm, (d) 750 µatm, (e) 750 µatm 12°C, (f) 1000 µatm, (g) 1000 µatm 12°C. Pole figures correspond to the calcite crystallographic orientation map colour key, gridlines represent 5° divisions of angular orientation. Note differences in the clustering and spread of the EBSD data provide information on the variability of the calcite crystal angles.

'scope for growth' limiting shell deposition as occurs in the bivalves *Crassostrea virginica* and *Mercenaria mercenaria*[8]. The impact of ocean acidification and sufficient feeding regimes on bioenergetics in juvenile somatic growth has been previously explored in *M. edulis*[16], where abundant food supply was found to maintain growth under increasing *p*CO₂. Sufficient food was supplied throughout the experimental culture during this study to ensure no effect of feeding regime on growth (See Materials and methods section: mus-
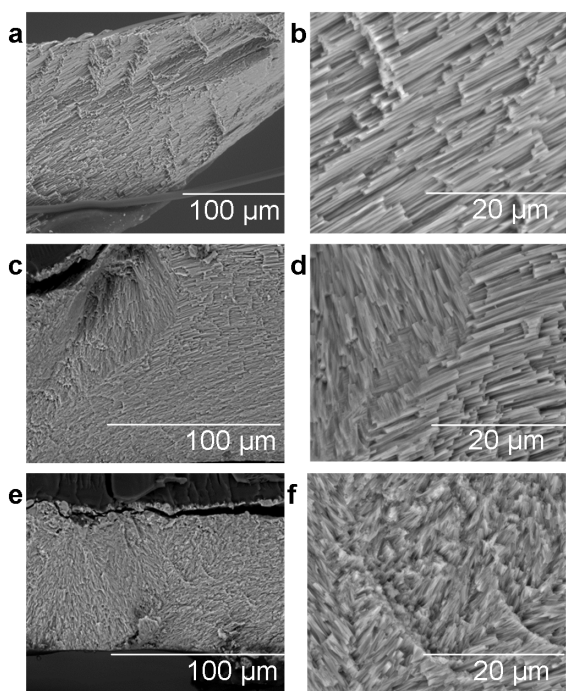
Figure 3 | Secondary electron images of new calcite growth in *M. edulis* shells after 6 months at 380, 750 and 1000 μatm pCO_2, all at ambient plus 2°C temperature, (a, b) 380 μatm, (c, d) 750 μatm, and (e, f) 1000 μatm, scale bars presented in μm. Images of uncoated samples acquired in environmental mode at 20 kV.

sel collection and culture). Changes to the degree of structural order of the calcite within the new shell growth could lead to reduced strength and softening of mussel shells reducing protection from predators and changing environments[8]. Reduced hardness in the calcitic oyster shells cultured under OA[8] could be attributable to disorientated calcite crystals as shown in new calcite growth in the mussel shells of this study.

There were significant shell growth reductions at 550 μatm pCO_2 (P = 0.050, t = −2.012, df = 27, n = 4) and 750 μatm pCO_2 (P = 0.050, t = −1.87, df = 27, n = 4) compared with the 380 μatm pCO_2 control (Figure 4). However, importantly, no significant differences in growth were observed between 380 and 1000 μatm pCO_2 treatments (Figure 4, P = 0.100, t = −1.410, df = 27, n = 4). Reductions in mollusc shell growth with increasing pCO_2 have similarly been observed in other mollusc species and studies[6,8,17]. Although in some cases carbonic anhydrase protein expression was reported as significantly enhanced in the isoform responsible for the hydrolysis of CO_2 to bicarbonate for biomineralisation[8].

Aragonite thickness within the shell was significantly reduced in mussels grown for 6 months under 550 μatm pCO_2 (Figure 4, P<0.050, t = −1.909, df = 27, n = 4) and 1000 μatm pCO_2 (Figure 4, P<0.010, t = −2.223, df = 27, n = 4) compared to the ambient experimental conditions at 380 μatm pCO_2. However, there was no difference in aragonite thickness between mussels grown at 380 and 750 μatm pCO_2 (P>0.100, t = 1.083, df = 27, n = 4) (Figure 4). Temperature had no significant effect on aragonite thickness in mussel shells (P>0.100, t = 0.426, df = 27, n = 4) (Figure 4). Potentially, at the less acidic ocean acidification scenarios, mussels will start to develop problems in maintaining new shell growth, however by the time 1000 μatm is reached there is potential for the mussels to continue to grow. Enhanced protein metabolism[6] and reduced organic component (chitin) availability for crystal formation (observed through down expression of genes relevant for chitin processing)[17] could explain differences in biomineral growth at 1000 μatm pCO_2.

Increasing pCO_2 did not have an effect on calcite thickness after 6 months exposure at 550 μatm pCO_2 (P>0.100, t = 0.673, df = 27, n = 4) nor 750 μatm pCO_2 (P>0.100, t = 0.248, df = 27, n = 4) (Figure 4). However, at 1000 μatm pCO_2 there was a significant increase in calcite thickness (P = 0.010, t = 2.199, df = 27, n = 4) relative to the calcite growth in ambient 380 μatm pCO_2 conditions (Figure 4). Ocean acidification combined with increased temperature had no significant effect on calcite growth (P>0.100, t = 0.691, df = 27, n = 4) (Figure 4). It would seem that mussels growing in future ocean acidification may maintain the ability to deposit calcite layers within the new shell, despite the disorientated crystal structure. Aragonite and calcite layers have very different mechanical properties, which is reflected in the micro-structure[8]. Aragonite crystals remained orientated in the 'brick wall' structure despite reductions in protein activity, whereas calcite crystals were disorientated as protein availability was reduced. In addition, up regulation in tyrosinase gene expression has been observed in *M. edulis* with increasing pCO_2 to 1120 μatm[17], it was suggested that tyrosinase, a critical enzyme in the formation of a proteinaceous layer involved in the periostracum maturation, is thought to represent a protective mechanism against external shell corrosion[17] which could explain the increased ability to produce calcite deposition.

Mantle tissue carbonic anhydrase activities were significantly reduced in mussels grown at 750 μatm pCO_2 for 6 months (P<0.05, t=−1.838, df=26, n=4) explaining the mussel shell growth reductions (Figure 5). No significant reductions in the mantle tissue carbonic anhydrase activities were observed at 550 μatm pCO_2 (P>0.05, t=−1.254, df=26, n=4) or 1000 μatm pCO_2 (P>0.05, t=−1.838, df=26, n=4) compared to the mussel grown at ambient levels of 380 μatm pCO_2 (Figure 5). Increasing temperature to ambient plus 2°C, did not produce significant changes in extrapallial fluid carbonic anhydrase protein activities (Mantle: P<0.05, t=−1.788, df=26, n=4. Extra pallial fluid: P>0.05, t=−0.297, df=26, n=4) (Figure 5). There was no significant effect of pCO_2 on the extrapallial fluid carbonic anhydrase activities at 550 μatm pCO_2 (P>0.05, t=0.421, df=26, n=4), 750 μatm pCO_2 (P>0.05, t=0.970, df=26, n=4) or 1000 μatm pCO_2 (P>0.05, t=1.256, df=26, n=4) (Figure 5). It would appear that mussels exposed to ocean acidification and increased temperatures maintain their ability to produce active carbonic anhydrase despite observed growth reductions and disorientated calcite crystal deposition. Carbonic anhydrase activity in the bivalves *Crassostrea virginica* and *Mercenaria mercenaria* appeared to remain constant with increasing pCO_2 when exposed for 15 weeks[8]. The findings of this current study suggest ocean acidification impacts the ability of mussels to deposit aragonite for new growth. Calcite deposition still occurs at the cost of the structural integrity of the shell in the form of disorientated calcite crystals. However, the biological response of mussels to produce carbonic anhydrase for biomineralisation remains unhindered by ocean acidification and increasing temperatures. Beyond 1120 μatm pCO_2, increases in metabolism reduce shell growth in *M. edulis*[6,17], however it has been suggested that, at lower pCO_2 values, the metabolism remains similar to the control levels, including the metabolism or recycling of proteins[8]. The reduced activity of mantle CA at 750 μatm, resulted in reduced growth. However, if reduced carbonic anhydrase activity also coincided with a maintained metabolism it could be suggested that the lower predicted pCO_2, could prove most detrimental to mussel growth. 750 μatm pCO_2 could potentially be a threshold for reduced mussel growth without the required stress-induced increases in oxygen consumption observed at ∼1000 μatm (1120 μatm)[6]. Molluscs have been thought to produce shells using carbonic anhydrase proteins to convert metabolically derived CO_2 to bicarbonate, but can also take bicarbonate directly from seawater[18]. The precise mechanisms are not fully understood which limits the ability to explain changes to mussel shell production.
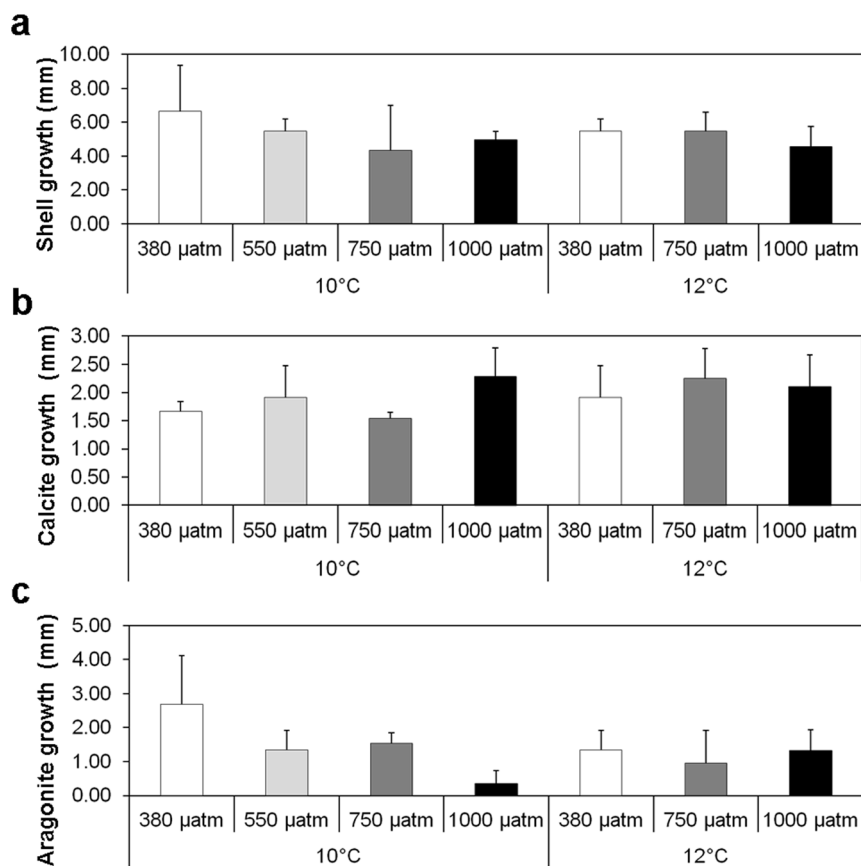
Figure 4 | Shell growth at 6 months experimental culture (mm). (a). Shell length increase for each pCO_2 and temperature. Error bars represent one standard deviation (n=4). (b). Calcite growth (mm) in mussel shells cultured for 6 months for each pCO_2 and temperature. Error bars represent one standard deviation (n=4). (c). Aragonite growth (mm) in mussel shells cultured for 6 months for each pCO_2 and temperature. Error bars represent one standard deviation (n=4).

Conclusion

Increasing exposure time to elevated pCO_2 can impact mussels' ability to control biomineralisation. There is potential that 750 µatm pCO_2 may be indicative of a potential threshold in ocean acidification impact for the mussel *M. edulis* with both reduced protein activity and shell growth. Increasing pCO_2 beyond 1000 µatm however has been observed to increase protein metabolism, chitinase mRNA and tyrosinase gene expression as a mechanism to support biomineralisation[17]. Such findings are in-keeping with increased CA production and continued calcite growth in *M. edulis* at 1000 µatm pCO_2. Although mussels appear to improve their ability to continue biomineralisation, this occurs at a cost to the structural integrity of the mussel shell. Changes in structural order could potentially impact the mussel shell strength and reduce protection from predators and changing environments. In order to project future implications of ocean acidification on marine calcifying organisms' biomineralisation mechanisms need to be fully understood. Further longer-term and possibly multi-generational experimental studies are also required to quantify the possibility of adaptation in marine calcifiers to future predicted climate change.

Methods

Mussel collection and culture. Mussels (*M. edulis*) were obtained from the Loch Fyne, Argyll, Scotland (Loch Fyne Oysters Ltd) during October 2012. Mussels were placed into experimental tanks (six L) supplied with natural filtered (1 µm and UV) seawater at Loch Fyne temperatures (7°C) and ambient pCO_2 (~380 µatm). Mussels were fed 10 ml of cultured microalgae (five species of zooplankton, *Nannochloropsis sp.*, *Tetraselmis sp.*, *Isochrysis sp.*, *Pavlova sp.*, *Thalassiosira weissflogii* (stock from Reefphtyo, UK,) ~2.8 million cellml^{-1}) per six L tank every other day. The feeding regime was conducted throughout the two week acclimation and experimental

period. This was sufficient to allow for growth under ocean acidification at 4666 cells ml^{-1} during culture[16]. To mark the start of the experimental period, mussels were placed into seawater containing the fluorescent dye calcein (150 µgL^{-1} Calcein C0875-25g Sigma-Aldrich) for six hours. Mussels were rinsed thoroughly in seawater, and placed back in experimental tanks. Each experimental tank contained 30 mussels; this was the appropriate number of mussels per six L experimental tank to maintain sufficient dissolved oxygen levels (tested prior to experiment).

Environmental conditions. Seasonal experimental temperatures and day length (light) mirrored those at the collection site. The Global warming scenario was 2°C above the natural temperature range of the controls which were changed each month according to measured Loch Fyne temperatures. Experiments were conducted at 380, 550, 750 and 1000 µatm pCO_2. Seawater pCO_2 concentrations were increased up to experimental levels (380, 550, 750 and 1000 µatm pCO_2) over a one month period. CO_2 was mixed into air lines supplying all experimental tanks[19]. Gas concentrations were logged continuously using LI-COR® Li-820 CO_2 gas analysers (Table 1). Seawater was topped up with a mixture of seawater and freshwater once a week to simulate fresh water pulses experienced by mussels in their natural environment. The seawater was filtered through a flow through filtration system including a V$_2$ power box in order to remove any ammonia, nitrate or nitrite accumulation within a week of water changes. Freshwater source addition for experimental culture would be comparable to that of Loch Fyne freshwater, accounting for changes in alkalinity. Seawater samples were collected in duplicate from three sites in Loch Fyne representing fluctuations in carbonate chemistry, these were measured for temperature, salinity, pH, dissolved oxygen (DO) and total alkalinity in order to calculate carbonate chemistry parameters (data presented Supplementary table 3). This is reflected in calcite (Ω Ca) and aragonite (Ω Ar) saturation states which are similar to other ocean acidification studies examining brackish water environments[6,20] and the natural variability present at the collection site (Table 1, supplementary table 3). Seawater salinity, temperature, and DO were checked daily and recorded once a week (YSI Pro2030). Seawater samples were collected (once per month) and spiked with 50 µl of mercuric chloride for subsequent total alkalinity (A$_T$) analysis via semi-automated titration (Metrohm 848 Titrino plus)[21] combined with spectrometric analysis using bromocresol indicator (Yao & Byrne, 1998) (Smart pH cuvettes, Ocean Optic Ltd) (Hach DR 5000™ UV-Vis). Certified seawater
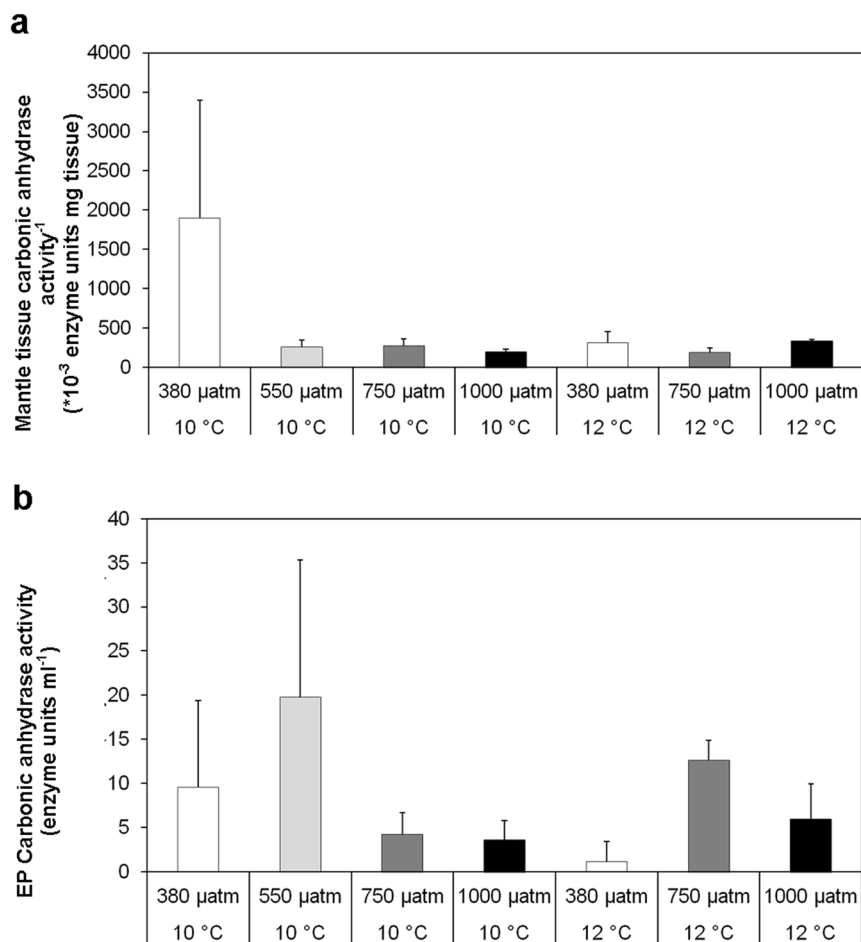
Figure 5 | Mussel average carbonic anhydrase activities for (a) mantle tissue (*10^{-3} enzyme units mg^{-1} of tissue) for each pCO$_2$ and temperature. (b) extrapallial fluid (EP) (enzyme units ml^{-1}) for each pCO$_2$ and temperature. Error bars represent one standard deviation (n=4).

reference materials for oceanic CO$_2$ (Batch 123, Scripps Institution of Oceanography, University of California, San Diego) were used as standards to quantify the error of analysis (Measured 2141 ± 54 μmolKg-1, CRM value 2225.21 ± 0.14 μmolKg-1)[21]. Seawater A$_T$, salinity, temperature and pCO$_2$ were used to calculate other seawater parameters using CO$_2$SYS[19,22] (Table 1).

Mussel sampling. Mussels were sampled at six months after the experimental acclimation period. Three mussels from each of four replicate tanks were removed and dissected for extrapallial fluids, mantle tissue and shells and stored frozen (−20°C) until analysis.

Carbonic anhydrase activity. CA activity was determined for the mantle tissue and extrapallial fluid from the posterior abductor muscle[23]. CA has already been observed in the acid-soluble matrices (ASMs) of the nacreous layer of mussel shells[24] and in mussel soft tissue[23] thus these areas were targeted. Mantle tissue and extrapallial fluid CA activity was determined by the colourimetric micromethod of analysis[23,25,26]. The activity units or enzyme units (EU) were calculated by the equation EU = (To-T)/T, where T and To are the reaction times for the pH change with and without the catalyst respectively[23]. Acetozolamide (3×10^{-4} M) was used as an inhibitor of the reaction, and added in place of Milli-Q water in order to observe reaction time without the functional catalyst[24].

Mussel shell growth. Shell growth and thickness of aragonite deposited since the calcein staining at the start of the experimental period, was measured using fluorescent microscopy (Olympus BH-2). Mussel shells were dried by incubation at 60°C for 48 hours, and then embedded in epoxy resin (EpoxyCure, Buehler) blocks. Embedded shells were sliced transversely using a diamond trim saw blade to section the whole length of the shell. Resin blocks were then polished. Calcein was detected under blue light excitation at 488 nm, where calcein fluoresces yellow-green[27,28]. Mussel shell growth (mm) was measured using microscope image analysis software (Microtec IS500 5MP camera software) as distance from stained calcein line to the tip of the new growth. Calcite and aragonite thickness was also measured (mm) using the microscope image analysis.

New calcite growth orientation. Mussel shells grown under ocean acidification culture for 6 months were examined under the Environmental Scanning Electron Microscope mode on the FEI Quanta 200F Environmental SEM. The shells were sectioned horizontally at the tip, snapped in the centre and laid on edge to reveal the calcite crystals on the broken edge secured upright in bees wax on a labelled microscope slide. Two individual mussel shells were imaged per treatment, the newest growth was used after the calcein staining to ensure only growth during experimental culture was measured. Crystal angles were determined using Image-J analysis, selecting 10 calcite crystals at random and determining the angle to the adjacent crystal.

Shell calcite crystal orientation. Calcite orientation of the crystals were examined using Electron Back Scatter Diffraction (EBSD) with a beam voltage of 20 kV under low vacuum mode (~50 Pa) on the FEI Quanta 200F Environmental SEM with the stage tilted to 70° to examine backscatter kikuchi patterns[29]. The mussel shells were cleaned and dried for 48 hours at 60°C before being embedded in epoxy resin as detailed in mussel shell growth methods. Resin blocks were polished by hand for 2–4 minutes using grit papers (P320, P800, P1200, P2500, and P4000), followed by further polishing for 4 minutes on cloths using 1 μ and 0.3 μ Alpha alumina, and 2 minutes using colloidal silica to reveal a smooth shell surface. Crystallographic orientation was imaged across the middle section of the length of mussel shell examining the calcite/aragonite interface. Crystallographic orientation maps were produced through OIM Analysis 6.2 software (Supplementary figure 1). EBSD results are presented as crystallographic pole figures and orientation maps with each colour representing a particular crystallographic orientation (confidence index <0.1 removed) (Figure 2 and Supplementary Figure 1). Pole figures were examined for spread of crystallographic orientation using 5 degree angle gridlines (Figure 2).

Statistical analysis. General linear model (GLM) ANOVA analyses in the platform R with RStudio were used to determine effects of temperature and pCO$_2$ on CA activity in extrapallial fluids and mantle tissues of mussels grown in experimental culture using four individual mussel replicates. Significant differences of temperature and pCO$_2$ on shell growth, calcite thickness and aragonite thickness of mussels grown under experimental conditions were also examined using GLM in the platform R

Table 1 | Experimental seawater chemistry parameters: salinity, dissolved oxygen (DO), pCO_2, total alkalinity (A_T ± standard deviation from the mean). Loch Fyne natural seawater chemistry parameters. Salinity, DO and temperature are averages collected manually throughout experiments, and pCO_2 given is the averaged values logged throughout the six months of experiments (logging every five minutes) using LI-COR® software. Bicarbonate (HCO_3^-) and carbonate (CO_3^{2-}), calcite saturation state (ΩCa), and aragonite saturation state (ΩAr) were calculated from measured parameters using CO_2Sys

Experimental condition	Salinity (ppt)	DO (%)	Temperature (°C)	pH_T	pCO_2 (µatm)	A_T (µmolkg⁻¹)	HCO_3^- (µmol kg⁻¹)	CO_3^{2-} (µmol kg⁻¹)	ΩCa	ΩAr
380 µatm Ambient	33 ± 1.4	96 ± 1.8	9.40 ± 0.36	7.7	376 ± 10	635 ± 29	590	12	0.29	0.18
380 µatm ambient plus 2°C	36 ± 1.5	98 ± 2.4	11.58 ± 0.69	7.7	376 ± 10	703 ± 79	642	17	0.39	0.25
550 µatm Ambient	33 ± 1.6	99 ± 2.2	10.01 ± 0.56	7.7	554 ± 63	971 ± 186	909	20	0.47	0.30
750 µatm Ambient	28 ± 4.1	99 ± 4.8	10.28 ± 0.34	7.5	769 ± 42	754 ± 55	726	8	0.21	0.13
750 µatm ambient plus 2°C	37 ± 3.8	98 ± 2.6	12.34 ± 0.43	7.4	769 ± 42	681 ± 42	649	9	0.21	0.13
1000 µatm Ambient	34 ± 4.6	99 ± 2.0	10.23 ± 0.40	7.3	1133 ± 32	698 ± 6	678	6	0.13	0.08
1000 µatm ambient plus 2°C	37 ± 2.1	98 ± 2.0	12.04 ± 0.35	7.2	1133 ± 32	642 ± 28	621	5	0.13	0.08
Loch Fyne Variability	19 ± 7.5	99 ± 13	15.70 ± 4.15	8.2	341 ± 103	1262 ± 416	1171 ± 430	34 ± 19	0.88 ± 0.47	0.52 ± 0.29
Loch Fyne (Lowest total alkalinity values)	18	116	12.80	8.1	251 ± 4	876 ± 13	798 ± 12	29.19 ± 0.44	0.68 ± 0.01	0.39 ± 0.01

using four individual mussel replicates. New calcite growth structural orientation angles were compared using means and standard deviation.

1. IPCC. *Climate change 2007: the physical science basis. Contribution of Working Group I to the Fourth Assessment Report of the Intergovernmental Panel on Climate Change* (eds Solomon S. *et al*) 996 pp (Cambridge University Press, 2007).

2. Doney, S. C., Fabry, V. J., Feely, R. A. & Kleypas, J. A. Ocean acidification: The other CO2 problem. *Ann Rev Mar Sci.* **1**, 169–192 (2009).

3. Beniash, E., Ivanina, A., Lieb, N. S., Kurochkin, I. & Sokolova, I. M. Elevated level of carbon dioxide affects metabolism and shell formation in oysters *Crassostrea virginica*. *Mar Ecol Prog Ser.* **419**, 95–108 (2010).

4. Byrne, M. Global change ecotoxicology: Identification of early life history bottlenecks in marine invertebrates, variable species responses and variable experimental approaches. *Mar Environ. Res.* **76**, 3–15 (2012).

5. Kamenos, N. A. *et al*. Coralline algal structure is more sensitive to rate, rather than the magnitude, of ocean acidification. *Glob. Change Biol.* doi: 10.1111/gcb.12351 (2013).

6. Thomsen, J. & Melzner, F. Moderate seawater acidification does not elicit long-term metabolic depression in the blue mussel *Mytilus edulis*. *Mar Biol.* **157**, 2667–2676 (2010).

7. Marin, F., Luquet, G., Marie, B. & Medakovic, M. Molluscan Shell Proteins: Primary Structure, Origin, and Evolution. *Curr Top Dev Biol.* **80**, 209–276. doi: 10.1016/S0070-2153(07)80006-8 (2008).

8. Ivanina, A. V. *et al*. Interactive effects of elevated temperature and CO2 levels on energy metabolism and biomineralization of marine bivalves *Crassostrea virginica* and *Mercenaria mercenaria*. *Comp Biochem Physiol.* Part A **166**, 101–111. doi: 10.1016/j.cbpa.2013.05.016 (2013).

9. Schmahl, W. W. *et al*. The microstructure of the fibrous layer of terebratulide brachiopod shell calcite. *Eur J Mineral.* **16**, 693–697. doi:10.1127/0935-1221/2004/0016-0693 (2004).

10. Pérez-Huerta, A. & Cusack, M. Common crystal nucleation mechanism in shell formation of two morphologically distinct calcite brachiopods. *Zool.* **111**, 9–15 (2008).

11. Roleda, M. Y., Boyd, P. W. & Hurd, C. L. Before ocean acidification: Calcifier chemistry lessons. *J. Phycol.* **48**, 840–843 (2012).

12. Fitzer, S. C. *et al*. Ocean acidification induces multi-generational decline in copepod naupliar production with possible conflict for reproductive resource allocation. *J. Exp. Mar. Biol. Ecol.* **418-19**, 30–36 (2012).

13. Kurihara, H. & Ishimatsu, A. Effects of high CO2 seawater on the copepod (Acartia tsuensis) through all life stages and subsequent generations. *Mar. Pollut. Bull.* **56**, 1086–1090 (2008).

14. Statistics and Information Service of the Fisheries and Aquaculture Department. *2010 FAO yearbook. Fishery and Aquaculture Statistics.* (eds Garibaldi, L. *et al*) 78 pp (Rome FAO, 2012).

15. Hahn, S., Rodolfo-Metalpa, R., Griesshaber, E., Schmahl, W. W., Buhl, D., Hall-Spencer, J. M., Baggini, C., Fehr, K. T. & Immenhauser, A. Marine bivalves geochemistry and ultrastructure from modern low pH experiments: environmental effect versus experimental bias. *Biogeosciences.* **9**, 1897–1914 (2012).

16. Thomsen, J., Casties, I., PAnsch, C., Körtzinger, A. & Melzner, F. Food availability outweighs ocean acidification effects on juvenile *Mytilus edulis*: laboratory and field experiments. *Glob Change Biol.* **19**, 1017–1027 (2013).

17. Hüning, A. K. *et al*. Impacts of seawater acidification on mantle gene expression patterns of the Baltic Sea blue mussel: implications for shell formation and energy metabolism. *Mar. Biol.* **160**, 1845–1861, doi: 10.1007/s00227-012-1930-9 (2013).

18. Roleda, M. Y., Boyd, P. W. & Hurd, C. L. Before ocean acidification: Calcifier chemistry lessons. *J. Phycol.* **48**, 840–843 (2012).

19. Findlay, H. S., Kendall, M. A., Spicer, J. I., Turley, C. & Widdicombe, S. Novel microcosm system for investigating the effects of elevated carbon dioxide and temperature on intertidal organisms. *Aquatic Biol.* **3**, 51–62 (2008).

20. Beldowski, J., Löfler, A., Schneider, B. & Joensuu, L. Distribution and biogeochemical control of total CO₂ and total alkalinity in the Baltic Sea. *J Mar Syst.* **81**, 252–259 (2010).

21. Dickson, A. G., Sabine, C. L. & Christian, J. R. *Guide to best practices for ocean CO₂ measurements* Vol. 3 (PICES Special Publication, 2007).

22. Riebesell, U., Fabry, V. J., Hansson, L. & Gattuso, J.-P. *Guide to best practices for ocean acidification research and data reporting* 260 pp (Publications Office of European Union, Luxembourg, 2010).

23. Medakovic, D. Carbonic anhydrase activity and biomineralization process in embryos, larvae and adult blue mussels *Mytilus edulis* L. Helgol. *Mar Res.* **54**, 1–6 (2000).

24. Marie, B. *et al*. Nacre calcification in the freshwater mussel *Unio pictorum*: carbonic anhydrase activity and purification of a 95 kDa calcium-binding glycoprotein. *ChemBioChem.* **9**, 2515–2523 (2008).

25. Maren, T. H. A simplified method for the determination of carbonic anhydrase and its inhibitors. *J. Pharmacol. Exp. Ther.* **139**, 140–153 (1960).

26. Bruns, W., Dermietzel, R. & Gros, G. Carbonic anhydrase in the sarcoplasmic reticulum of the rabbit skeletal muscle. *J. Physiol.* **371**, 351–364 (1986).

27. Mahé, K., Bellamy, E., Lartaud, F. & de Rafélis, M. Calcein and manganese experiments for marking the shell of the common cockle (Cerastoderma edule):

tidal rhythm validation of increments formation. *Aquat Living Resour.* **23**, 239–245 (2010).

28. Tambutté, E. *et al.* Calcein labelling and electrophysiology: insights on coral tissue permeability and calcification. *Proc. R. Soc. B.* **279**, 19–27 (2012).

29. Pérez-Huerta, A. & Cusack, M. Optimizing electron backscatter diffraction of carbonate biominerals—resin type and carbon coating. *Microsc Microanal.* **15**, 197–203, doi:10.1017/S1431927609090370 (2009).

Acknowledgments

Author contributions

V.R.P., N.A.K. and M.C. conceived the original study and secured funding. S.C.F., V.R.P., M.C. and N.A.K. designed the experiments. S.C.F. performed experiments, analysed data and wrote the manuscript with input from V.R.P., N.A.K. and M.C. all of whom provided technical support and conceptual advice.

Additional information

Supplementary information accompanies this paper at http://www.nature.com/scientificreports

Competing financial interests: The authors declare no competing financial interests.